Electronic structure of hydrogenated fluorinated amorphous GaAs alloys

Bal K. Agrawal and Savitri Agrawal
Department of Physics, Allahabad University, Allahabad 211 002, Uttar Pradesh, India
(Received 23 January 1986)

The electronic structure of amorphous GaAs:H:F alloys is discussed by using a cluster—Bethe-lattice method. The various hydrogenated and fluorinated conformations, e.g., GaF, GaF_2, GaF_3, AsF, AsF_2, AsF_3, GaH, GaH_2, GaH_3, AsH, AsH_2, AsH_3, AsFH, AsF_2H, $AsFH_2$, GaFH, GaF_2H, and $GaFH_2$ in *a*-GaAs have been investigated. Along with the features seen earlier in the elemental semiconducting alloys like *a*-Si:F:H and *a*-Ge:F:H alloys, novel peaks are seen to arise from dangling bonds as well as from the incorporated H atoms. Photoemission and other types of experiments are greatly needed to detect the predicted structure in the *a*-GaAs alloys.

I. INTRODUCTION

The III-V compounds such as GaAs, GaP, and GaSb are direct-band-gap semiconductors exhibiting efficient electron-hole radiative recombination. High carrier mobilities found in them has spurred tremendous efforts in the development of high-speed GaAs digital circuits with very low power consumption for application in the computer industry.

In the present paper, we make a detailed study of the electronic structure of the hydrogenated and fluorinated amorphous GaAs alloys by using a cluster—Bethe-lattice method (CBLM). Previous applications of this method[1–8] were quite successful in terms of understanding the electronic and vibrational excitations of the elemental semiconductor alloys like *a*-Si:F:H and *a*-Ge:F:H.

Section II contains a very brief account of the theory, and the results are contained in Sec. III. The conclusions are included in Sec. IV.

II. THEORY

The linear combination of atomic orbitals (LCAO) method in a Bethe lattice has been used for the calculation of the density of states. The local Green's function at any site can be calculated exactly. The density of states of the Bethe lattice for the host matrix is smooth and featureless, and therefore the local environment of the atoms in the cluster leaves signatures on the density of the electronic energy states. The localized states induced by the cluster of atoms outside the bulk electron bands appear as peaks of delta-function type. On the other hand, the induced states lying within the bulk band (resonance states) acquire finite width. For details, we refer to our earlier papers.[3–5] The local density of states at the atomic site i is given by

$$\rho_i(E)=\left[-\frac{1}{\pi}\right]\mathrm{Im\,Tr}\,|\,\underline{G}_{ii}(E)\,|\ ,$$

where $\mathrm{Im\,Tr}(\underline{G}_{ii})$ is the imaginary part of the trace of the local Green's function matrix at site i for energy E.

TABLE I. Atomic orbital energies (in eV). The energies have been measured with respect to the top of the valence band.

Orbital	Ga	As	F	H
E_p	3.82	−0.19	−9.28	
E_s	−2.87	−8.83	−28.08	−3.38
	(−3.65)[a]	(−9.61)[a]		

[a]Atomic values, Ref. 11.

III. CALCULATION AND RESULTS

We consider the nearest-neighbor and the second-nearest-neighbor interactions for the As—F, As—H, Ga—F, Ga—H, F—F, and H—H bonds. The electrons of each atom are described by one s orbital and three p orbitals (p_x,p_y,p_z). One needs to know the six interaction integrals E_s, E_p, U, X, V, and T for each type of bond. Here E_s and E_p are the term values for the atomic s and p orbitals and the interatomic interaction integrals between (s,p_x,p_y,p_z) at one site and (s',p_x',p_y',p_z') at the other site are given by

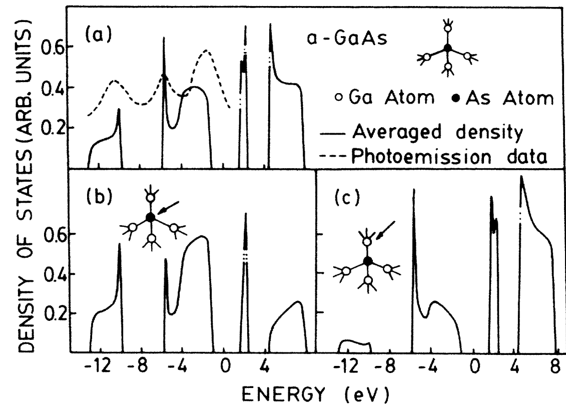

FIG. 1. (a) Comparison of the calculated averaged electronic density of states for *a*-GaAs with the photoemission data of Ref. 9, (b) local density at As atom, (c) local density at Ga atom. In all the figures arrows indicate the atoms at which the local density has been calculated.

 ©1986 The American Physical Society

TABLE II. Values of the first- and second-neighbor matrix elements for the different bonds in eV.

Interactions	Bond	U	X	V	T
First neighbor	Ga—As	−1.78	0.93	1.59	0.61
	Ga—F	−8.664	2.70	3.43	0.313
	Ga—H	−3.157	1.202		
	As—F	−8.664	2.70	3.43	0.313
	As—H	−3.157	1.202		
Second neighbor	H—H	0.469			
	H—Ga	0.3224	0.000		
	H—As	0.3224	0.00		
	F—F	3.191	−0.12	0.782	0.552
	F—H	1.83	−0.06		
	F—Ga	1.596	−0.0597	0.271	0.2023
	F—As	1.596	−0.0597	0.271	0.2023

TABLE III. Calculated peak positions for the T_3^0, T_2^0, T_1^0 defects in a-GaAs alloys measured in eV. The asterisk denotes the atom at which the local density of state has been calculated. The uncoupled lines at one end in the first and third columns represent the dangling bonds.

Dangling bonds	Peak position		Dangling bonds	Peak position	
$-$As*Ga_3		−0.8	$-$Ga*As_3	0.85	
$=$As*Ga_2	−9.70	−0.2	$=$Ga*As_2	0.0,	3.9
$\equiv$As*Ga	−9.35	−0.2	$\equiv$Ga*As	0.90,	3.9

TABLE IV. Calculated H-induced peak positions for the different hydrogenated complexes in a-GaAs alloys measured in eV.

Complex	Peak position	Complex	Peak position
AsH	−11.8 (As)	GaH	−11.2 (Ga)
	−4.0 (H)		−6.7 (H)
	−2.6 (As)		−3.5 (H)
	0.8 (H)		−3.2 (Ga)
AsH_2	−12.2 (As)	GaH_2	−10.6 (Ga)
	−5.2 (H)		−7.5 (H)
	−2.8 (As)		−4.6 (H)
	0.9 (H)		−2.8 (Ga)
			2.8 (H)
AsH_3	−12.4 (As)	GaH_3	−10.2 (Ga)
	−5.0 (H)		−8.1 (H)
	−2.8 (As)		−4.6 (H)
	1.0 (H)		−2.4 (Ga)

TABLE V. Calculated F-induced peak positions for the different fluorinated complexes in a-GaAs alloys measured in eV.

Complex	Calculated peak	Complex	Calculated peak
AsF	−13.0 (F)	GaF	−12.8 (F)
	−10.4 (F)		−10.2 (F)
	−7.2 (F)		−9.6 (F)
	−1.2 (As)		−3.0 (Ga)
AsF_2	−13.4 (F)	GaF_2	−13.0 (F)
	−11.0 (F)		−10.6 (F)
	−9.5 (F)		−9.8 (F)
	−9.2 (F)		−9.2 (F)
	−1.0 (As)		−2.2 (Ga)
AsF_3	−13.6 (F)	GaF_3	−13.4 (F)
	−11.6 (F)		−11.1 (F)
	−11.0 (F)		−10.6 (F)
	−10.0 (F)		−9.8 (F)
	−9.4 (F)		−9.4 (F)
	−8.8 (F)		−8.4 (F)
	−1.2 (As)		−2.0 (Ga)

TABLE VI. Calculated peak positions for the different hydrogenated fluorinated complexes in a-GaAs in eV.

Complex	Peak position	Complex	Peak position
AsFH	−13.2 (F)	GaFH	−12.4 (F)
	−10.4 (F)		−10.0 (F)
	−7.8 (F,H)		−5.8 (H)
	−1.2 (As)		−2.4 (Ga)
AsF_2H	−13.6 (F)	GaF_2H	−13.0 (F)
	−11.0 (F)		−10.6 (F)
	−10.4 (F)		−9.8 (F)
	−9.2 (F)		−9.2 (F)
	−6.4 (H)		−5.2 (H)
	−1.2 (As)		−2.0 (Ga)
$AsFH_2$	−13.4 (F)	$GaFH_2$	−12.2 (F)
	−10.4 (F)		−10.0 (F)
	−8.2 (F)		−6.2 (H)
	−5.3 (H)		−4.4 (H)
	−4.8 (H)		−2.0 (Ga)
	−1.8 (As)		

$$\langle s\,|H|\,s'\rangle = U,\ \ \langle s\,|H|\,p'\rangle = X\ ,$$

$$\langle p_x\,|H|\,p_x'\rangle = V,\ \ \langle p_x\,|H|\,p_y'\rangle = T\ .$$

The values of the interaction parameters for all the bonds have been scaled with the help of corresponding parameters in Si:F:H alloys[4,5] using a $1/d^2$ law, where d is the bond length. The parameters used in the present calculations are shown in Tables I and II.

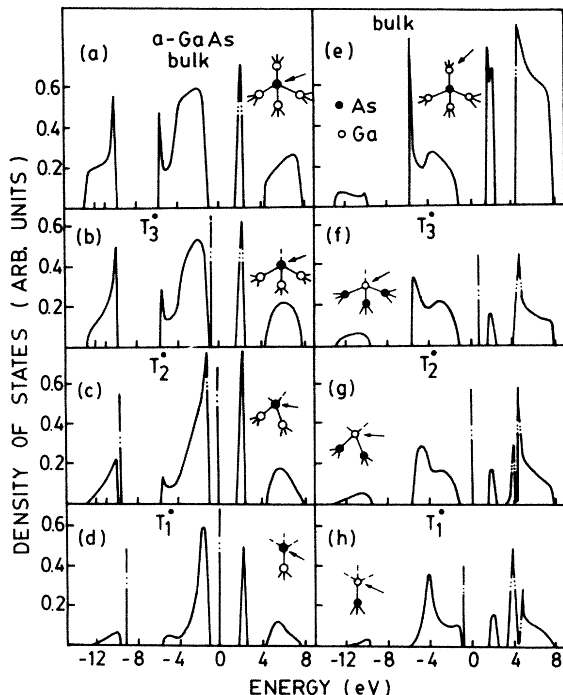

FIG. 2. Calculated local electronic density of states for different defects in a-GaAs alloys. (a) Density at As atom in bulk GaAs. (b) Density at As having one dangling bond. (c) Density at As with two dangling bonds. (d) Density at As with three dangling bonds. (e)—(h) are similar to (a)—(d) but for Ga atoms.

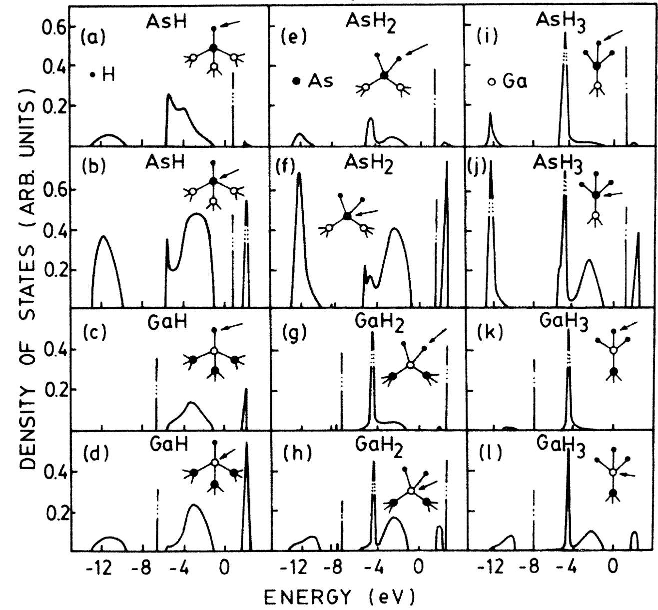

FIG. 3. Calculated local electronic density of states for the hydrogenated amorphous GaAs alloys. (a)—(d) Local densities at H, As, and Ga atoms for monohydrides. (e)—(h) Corresponding local densities for dihydrides. (i)—(l) Local densities for trihydrides.

The computed electronic density of states averaged over the Ga and As atoms in bulk GaAs has been compared with the photoemission data[9] in Fig. 1(a). The local density of states at the constituent atoms is depicted in Figs. 1(b) and 1(c).

The three peaks at −10.0, −6.0, and −2.0 eV in the valence-band region in the computed density of states appearing at the band edges are in excellent agreement with the photoemission peaks.[9,10] The two peaks at −10.0 and −2.0 eV originate mainly from the s and p orbitals of the As atom whereas the middle peaks near −6.0 eV from those of the Ga atom. The computed electronic energy gap is 2.0 eV, a value which is somewhat greater than the actually measured energy gap of a-GaAs. This widening of gap in a Bethe lattice has also been seen in all the earlier calculations performed for a-Si or a-Ge. However, the calculated ionic gap of about 4.2 eV is surprisingly in good accord with the measured one.

A. T_n defect ($n=1,3$)

The local density of states on Ga and As atoms in bulk GaAs and for the isolated T_3^0, T_2^0, and T_1^0 defects is depicted in Fig. 2. The dangling bond states at As atoms appear in the low-energy region in contrast to those of Ga which appear in comparatively high-energy region (Table III). For the single bond (T_3^0-defect) at an As atom [Fig. 2(b)], there appears a dangling bond state in the gap near the top of the valence band at −0.8 eV. For the double and triple dangling bonds at As [Figs. 1(c) and 1(d)], one finds states both in the fundamental-gap and ionic-gap regions appearing at −0.2 and −9.5 eV, respectively. This behavior of large splitting in the multiple dangling bonds

is quite different from what was earlier observed in *a*-Si or *a*-Ge where the split dangling bond states were confined more or less to the fundamental gap.

For the T_3^0 defect at Ga atom [Fig. 1(f)], one observes a single gap state at 0.85 eV. For the T_2^0 and T_1^0 defects [Figs. 1(g) and 1(h)], dangling bond states in the fundamental gap appear at 0.0 and -0.9 eV, respectively, and in the valence band region at the same location (3.9 eV).

B. H_n or F_n, $n=1,2,3$ units in *a*-GaAs

The computed local electron density of states for the H (F) atoms coupled to the cation (Ga) and anion (As) ions has been shown in Figs. 3 and 4, respectively. The units considered are the mono-, dia-, and trihydrides (fluorides). Tables IV and V contain the locations of the H (F-) induced peaks.

It is noted that, along with the structure seen earlier in the elemental *a*-Si:H and *a*-Ge:H semiconducting alloys, with the incorporation of H atoms one observes some new peaks in the ionic gap and also in the fundamental gap just near the bottom of the conduction band of *a*-GaAs. The Ga—H bonds incur extra states in the ionic gap whereas the As—H bonds incur states just below the bottom of the conduction band.

All the F-atom induced states are *p*-like states (Table V) and appear in the low-energy region. It is noted that there is a large depletion of density of states in the region of the top of the valence band and the bottom of the conduction band by the presence of H or F atoms.

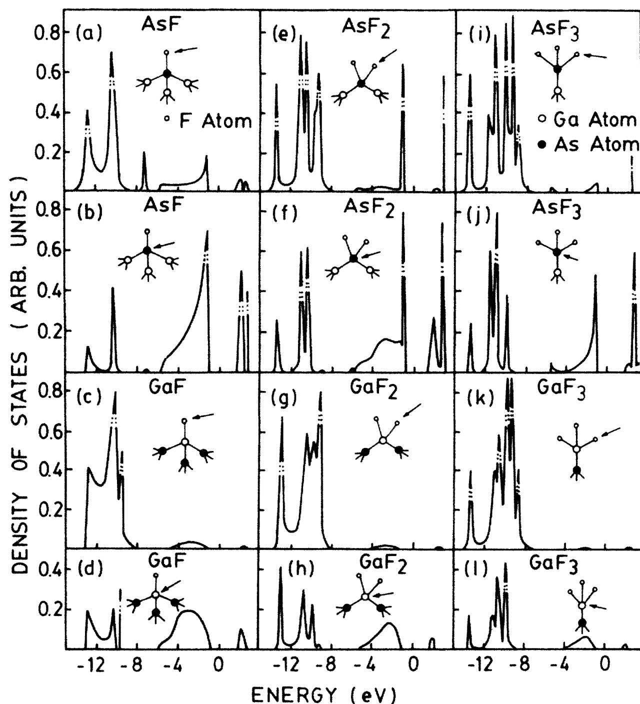

FIG. 4. Same as for Fig. 3 but for mono-, di-, and trifluorides.

C. (Ga or As)F_mH_n complexes in *a*-GaAs

For the mixed F and H atoms complexes like (Ga or As)FH, (Ga or As)F_2H, and (Ga or As)FH_2, the computed local density of states at the various types of the atoms is shown in Fig. 5. Almost all the F- and H-induced states in the mixed complexes appear. However, their locations seen earlier in the purely hydrogenated (*a*-GaAs:H) or in the fluorinated (*a*-GaAs:F) alloys are slightly altered (Table VI). The changes incurred by the H atoms on the F-induced peaks lying near the bottom of the valence band are quite small. However, the shifting of peaks is quite appreciable both for the H- and F-induced peaks in the high-energy region of the valence band.

IV. CONCLUSIONS

The features incurred by the incorporated H and F atoms in the electronic density of states of GaAs matrix are very similar to those seen earlier in the elemental semiconductor alloys like *a*-Si:F:H and *a*-Ge:F:H alloys. However, there also appear novel states due to the isolated T_3^0, T_2^0, and T_1^0 defects in the ionic bandgap as well as in the fundamental bandgap in GaAs. Extra peaks also ap-

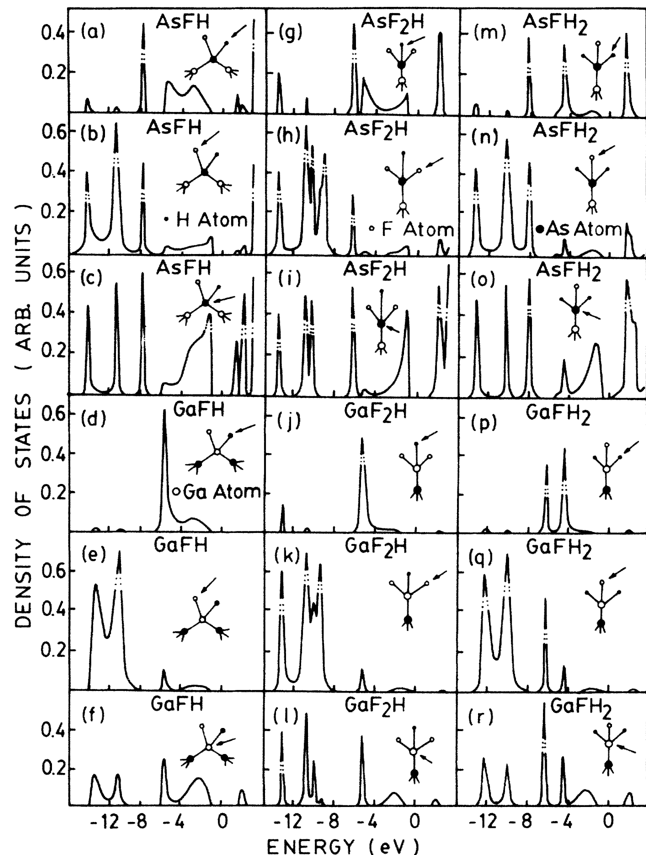

FIG. 5. Calculated local electronic density of states for the various F and H complexes in amorphous GaAs alloy. (a)—(c) Densities at H, F, and As atoms for AsFH complex. (d)—(f) Densities at H, F, and Ga atoms for GaFH complex. (g)—(l) Corresponding densities for AsF_2H and GaF_2H complexes. (m)—(r) Densities for $AsFH_2$ and $GaFH_2$ complexes.

pear in the valence band, fundamental gap, and the conduction-band region because of the coupling of H atoms to the Ga ions. Photoemission and other experiments need to be performed on hydrogenated and fluorinated GaAs alloys to detect the predicted structure in the electronic density of states.

ACKNOWLEDGMENTS

The authors are thankful to the Department of Science and Technology, the Government of India and to the University Grants Commission (New Delhi, India) for financial support.

[1]D. Weaire and M. F. Thorpe, Phys. Rev. B **4**, 2508 (1971); D. Weaire, Phys. Rev. Lett. **26**, 1541 (1971).

[2]F. Yndurain, and J. D. Joannopoulos, Phys. Rev. B **11**, 2957 (1975); J. D. Joannopoulos and F. Yndurain, *ibid.* **10**, 5164 (1974).

[3]B. K. Agrawal, Phys. Rev. Lett. **46**, 774 (1981).

[4]B. K. Agrawal and S. Agrawal, Phys. Rev. B **29**, 6870 (1984).

[5]S. Agrawal and B. K. Agrawal, Phys. Rev. B **31**, 5355 (1985).

[6]B. K. Agrawal and B. K. Ghosh, J. Phys. C **18**, 3897 (1985).

[7]B. K. Ghosh and B. K. Agrawal, Phys. Rev. B **33**, 1250 (1986).

[8]Savitri Agrawal and Bal K. Agrawal, J. Phys. C (to be published).

[9]L. Ley, R. A. Pollak, F. R. McFeeley, S. P. Kawalcyzk, and D. A. Shirley, Phys. Rev. B **9**, 600 (1974).

[10]C. Senemaud, E. Belin, A. Gheorghiu, and M. L. Theye, J. Non-Cryst. Solids, **77&78**, 1289 (1985).

[11]S. Froyen and W. A. Harrison, Phys. Rev. B **20**, 2420 (1980).